Food Chemistry 395 (2022) 133587

Contents lists available at ScienceDirect

Food Chemistry

journal homepage: www.elsevier.com/locate/foodchem

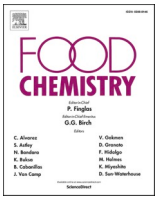

Wine astringent compounds monitored by an electrochemical biosensor

Joana J. Costa [a,b,c], Felismina T.C. Moreira [a,c], Susana Soares [d], Elsa Brandão [d], Nuno Mateus [d], Victor De Freitas [d], M. Goreti F. Sales [a,b,c,*]

[a] BioMark@ISEP, School of Engineering of the Polytechnic Institute of Porto, Porto, Portugal
[b] BioMark@UC, Department of Chemical Engineering, Faculty of Sciences and Technology, Coimbra University, Coimbra, Portugal
[c] CEB/LABBELS, Center of Biological Engineering, Minho University, Braga, Portugal
[d] LAQV-REQUIMTE, Departamento de Química e Bioquímica, Faculdade de Ciências da Universidade do Porto, Porto, Portugal

ARTICLE INFO

Keywords:
Polyphenols
Proline Rich Protein
α-Amylase
Screen-printed electrodes
Astringent compounds
Electrochemical biosensor

ABSTRACT

An innovative approach for monitoring astringent polyphenols in beverages (wines) is described, consisting of an electrochemical biosensor constructed by adsorbing salivary α-amylase or proline-rich protein (PRP) onto amined gold screen-printed electrodes. Interaction with polyphenols was tested using pentagalloyl glucose (PGG) as a standard, an important representative element for astringency. The analytical properties of the resulting biosensors were evaluated by electrochemical impedance spectroscopy at different pHs. The PRP-biosensor was able to bind to PGG with higher sensitivity, displaying lower limit of the linear range of 0.6 μM. Wine samples were tested to prove the concept and the concentrations obtained ranged from 0.17 to 4.7 μM, as expressed in PGG units. The effects of side-compounds on PRP and on α-amylase binding to PGG were tested (gallic acid, catechin, ethanol, glucose, fructose and glycerol) and considered negligible. Overall, concentrations > 1.0 μM in PGG units are signaling electrochemical impedance, providing a quantitative monitoring of astringent compounds.

1. Introduction

Polyphenols are secondary metabolites of plants and are therefore found in all plant products. These compounds range from simple structures such as phenolic acids to very complex molecules such as the hydrolysable tannins. These compounds are classically divided into the main families of non-flavonoids and flavonoids. The non-flavonoid family includes phenolic acids, stilbenoids and lignans. The flavonoid family is larger and includes anthocyanins, flavanols, flavones, flavanones and isoflavones. Tannins is another common name for some polyphenols that have the special property of interacting with and precipitate proteins (Bate-Smith & Swain, 1962). Tannins are also divided into two major families: condensed and hydrolysable tannins. The former are oligomers or polymers of flavanols with structural units of (*epi*-)catechin, and the later are monosaccharide esters of glucose with gallic acid or ellagic acid.

One of the most worldwide known property of these compounds are the health benefits linked to their moderate consumption. Nevertheless, besides their positive health effects, polyphenols can have also a negative impact when consumed at high concentrations. Within the negative impacts there are the inhibition of digestive enzymes leading to impairment of digestion and nutrients absorption or kidney/liver damage (Cory, Passarelli, Szeto, Tamez, & Mattei, 2018). In fact, as a countermeasure to their potentially harmful effects and intake, the organoleptic properties linked to some polyphenol's are unpleasant, namely astringency and bitterness. On the other hand, this can also compromise their consumption at moderate concentrations and impair the positive health effects (Canon, Neiers, & Guichard, 2018; Huang & Xu, 2021; Ma, Guo, Zhang, Wang, Liu, & Li, 2014; Susana Soares, Brandão, Mateus, & de Freitas, 2017). These unpleasant taste properties of polyphenols are a real challenge for the food industry. The food industry has made efforts to reduce the content of astringent/bitter tasting compounds (Huang & Xu, 2021), which compromises the potential health benefits of foods. On the other hand, there are also foods where astringency and bitterness are a newly introduced problem. These are either functional foods enriched with health-promoting (but bitter and astringent) polyphenols, or healthy foods with reduced sugar/fat/salt content developed due to health concerns related to obesity, diabetes

* Corresponding author at: Chemical Engineering Department of the Faculty of Sciences and Technology of the University of Coimbra, Rua Silvio Lima, Polo II, Coimbra, Portugal.
E-mail addresses: goreti.sales@eq.uc.pt, goreti.sales@gmail.com (M.G.F. Sales).

https://doi.org/10.1016/j.foodchem.2022.133587
Received 4 December 2021; Received in revised form 30 May 2022; Accepted 25 June 2022
Available online 27 June 2022

and cardiovascular disease. (Goldberg, Grant, Aliani, & Eskin, 2017; Liem, Miremadi, & Keast, 2011; Nadathur & Carolan, 2017). Therefore, it is particularly important for the food industry to find out which polyphenols are astringent or bitter, which mechanisms are behind these taste properties and how to modulate them without removing the healthy compounds.

The molecular perception of bitterness is relatively well understood. Bitter taste is perceived through the activation of bitter receptors (TAS2Rs) (Meyerhof et al., 2010; Upadhyaya, Singh, Bhullar, & Chelikani, 2017). TAS2Rs are members of the G-Protein family and are seven-transmembrane receptors. In oral cavity, they are expressed at the surface of taste buds. Humans express only 25 TAS2Rs for detection of hundreds of structurally diverse bitter molecules (Meyerhof, Born, Brockhoff, & Behrens, 2011). The TAS2Rs activated by some polyphenols have been recently identified and some of them seem to be specific for polyphenols, such as TAS2R5, TAS2R7, TAS2R14 and TAS2R39 (Roland et al., 2013; Susana Soares, Kohl, Thalmann, Mateus, Meyerhof, & De Freitas, 2013).

In contrast, the molecular origin of astringency is not yet fully understood, and the connection or contribution of the various proposed mechanisms is still unknown (Canon et al., 2018; Huang & Xu, 2021; Schöbel et al., 2014; Susana Susana Soares et al., 2017). The most widely accepted mechanism is based on the precipitation of salivary proteins by polyphenols, especially proline-rich proteins (PRPs). PRPs are an important group of proteins in this field, being divided into different classes: acidic, basic and glycosylated PRPs. PRPs strongly associated with astringency are mostly basic and acidic (Canon et al., 2013; Quijada-Morín, Crespo-Expósito, Rivas-Gonzalo, García-Estévez, & Escribano-Bailón, 2016; Susana Soares, Soares, Brandão, Guerreiro, Mateus, & de Freitas, 2020). Besides PRPs, other relevant salivary protein families that have been also linked to astringency include as α-amylase (Guerreiro, Freitas, Sutherland, & Sales, 2012) or statherin, P-B peptide, mucins (Davies et al., 2014; Ployon et al., 2018; Silva, García-Estévez, Brandão, Mateus, de Freitas, & Soares, 2017) and histatins (Yan & Bennick, 1995).

Although it is known that some compounds perceived as astringent (e.g., aluminum sulfates vulgo alums) are unable to precipitate salivary proteins (Breslin, Gilmore, Beauchamp, & Green, 1993; de Wijk & Prinz, 2005), this is not the case for polyphenols. The interaction of polyphenols with salivary proteins, forming both soluble and insoluble complexes, has been widely published and recognized (Huang & Xu, 2021). Although it is difficult to assign general astringency and astringency descriptors for all astringent compounds to a single physicochemical phenomenon, interaction with salivary proteins is a key phenomenon for the astringency of polyphenols. Although information about astringency in foods remains very important, the food industry still lacks a meaningful and effective method to evaluate it, and trained sensory panels are routinely used for this purpose. However, sensory impressions of astringency are easily confused with bitterness and require specialized and extensive training to reliably distinguish between them. All of these aspects are time-consuming and costly. Some taste sensors already exist (e-tongues), they are usually made from modified polymer electrodes, and the results show that what works for one compound does not work for the other. Furthermore, these existent physicochemical sensors perform well in simple test systems (e.g., one compound alone) and for known molecules. At the end, these sensors are in many cases only of limited value because they are based on very different physicochemical mechanisms compared to the physiological mechanisms. The most specific biosensors are the ones using the biological functional components of taste properties as sensitive elements. There are already some prototype taste sensors, but their relation to human perception of astringency remains limited, which complicates their application in the food industry (Zhang, Wei, Fan, Zhou, & Liu, 2020). There are also other biosensors that do not test however the interaction involving PRPs (Guerreiro et al., 2014; Guerreiro, Sutherland, Freitas, & Sales, 2013; Guerreiro, Teixeira, Freitas, Sales, & Sutherland, 2017) that is considered of great relevance nor involve devices that may be able to operate in routine procedures. So, specific, reliable and high-throughput sensors involving interactions with PRPs are still an emerging necessity. The use of electrochemical sensors to implement this approach is also an advantage in terms of cost and rapidity, also offering the possibility to carry out analysis in situ, where required. Overall, studies made with electrochemical detection and PRP binding for monitoring astringent compounds is a major novelty in this field.

Therefore, the main objective of this work was to develop an electrochemical biosensor based on the electrostatic affinity between polyphenols and salivary proteins (α-amylase and PRP), to test whether it could be useful for measuring the presence of pure astringent compounds and possibly complex food matrices. This affinity was tracked by electrical changes in the typical behavior of a standard iron redox probe monitored by cyclic voltammetry (CV) and electrochemical impedance spectroscopy (EIS). Using an electrochemical-based device with 3-printed electrodes, the food analysis may take place outside the laboratory and provide responses in-situ within less than 1 h.

2. Experimental section

2.1. Apparatus

Electrochemical measurements were conducted in a potentiostat/galvanostat from Metrohm Autolab/PGSTAT302N, impedimetric module and controlled by Nova software. The gold screen-printed electrodes (Au-SPEs) were purchased from Metrohm (DRP-250AT), with working and counter electrode made of gold and reference electrode and electrical contacts made of silver. For the electrochemical studies, the screen-printed electrodes (SPEs) were inserted into a DropSens switch box, which connected the electrical contacts of the Au-SPEs to the electrical terminals of the potentiostat/galvanostat.

2.2. Reagents and solutions

All chemicals were of analytical grade and the water was ultra-pure Milli-Q laboratory water. Potassium hexacyanoferrate III ($K_3[Fe(CN)_6]$), potassium hexacyanoferrate II ($K_4[Fe(CN)_6]$) Trihydrate and o-phosphoric acid 85% (H_3PO_4) was purchased from Riedel-deHäen, Porto Salvo; phosphate-buffered saline (PBS, 0.01 mol/L, pH 7.4) was purchased from Panreac. AppliChem; cysteamine hydrochloride (Cys), L-cystine, thiomalic acid (TA) were purchased from Merck Life Science S. L.U. sucursal em Portugal); sulfuric acid was purchased from BDH®; α-amylase from human saliva (≥98%) and gallic acid (GA) (≥97%) were purchased from Sigma-Aldrich, Saint Louis.

Fresh solutions of 50 μg/mL Cys, TA and L-cysteine were prepared in deionized water. Electrochemical assays were performed with 5.0×10^{-3} mol/L solutions of $K_3[Fe(CN)_6]^{4-}$ and $K_4[Fe(CN)_6]^{3-}$ in PBS buffer. PGG (19 μg/mL) and PRP (250 μg/mL) solutions were prepared in PBS buffer with pH 5.0 or 7.4 and stored at 4 °C. The solution of α-amylase (250 μg/mL) was prepared in acetate buffer at pH 5.0 or 7.4.

2.3. PGG

PGG was synthesized from tannic acid according to the method of Chen and Hagerman (Chen, Hagerman, & Minto, 2003). Briefly, 5.0 g of tannic acid (Fluka, BioChemika, Switzerland) was dissolved in a solution of 70% methanol in acetate buffer (0.1 mol/L, pH 5.0) at 65 °C for 15 h, and the pH of the solution was determined. After this time, the pH of the mixture was immediately adjusted to 6.0 with NaOH. The methanol was evaporated, and the resulting suspension was extracted with 3 volumes of diethyl ether and 3 volumes of ethyl acetate. The ethyl acetate extracts were combined and evaporated. The resulting suspension was centrifuged, and the precipitate was redissolved by heating in a 2% methanol solution. After cooling the solution to room temperature, the

PGG precipitated and was collected by centrifugation. The PGG was washed twice with ice-cold 2% methanol solution and once with ice-cold distilled water. The final material was freeze-dried to obtain a white powder with a total mass yield of 23%. The purity of the obtained PGG was determined by HPLC analysis and ^{1}H NMR spectroscopy.

2.4. PRpP

Acidic PRPs (aPRPs) were isolated from human saliva. Saliva was isolated and stabilized as reported previously (Susana Soares et al., 2011). Saliva was isolated from different volunteers and subjected to acid extraction with 10% TFA (final concentration = 0.1%) (Sigma-Aldrich, Germany) to obtain protein content by inhibiting intrinsic proteases and to precipitate some salivary proteins with high molecular weight (such as α-amylases, mucins, carbonic anhydrase and lactoferrin). This acid saliva is rich in several salivary peptides, namely histatins, PRPs, statherins and cystatins. After mixing the acid saliva, the samples were centrifuged (8000g, 5 min) and the supernatant was obtained. This supernatant was dialyzed at 4 °C with agitation against acidic water (pH 3.5) (cellulose membrane, MWCT 3.5 kDa) until the ionic strength was reduced to low and stable values (fresh water was replaced several times). Subsequently, this saliva was centrifuged again, and the supernatant was freeze-dried. The resulting powdered saliva was dissolved in the smallest possible amount of water and filtered. The resulting solution was separated into the different families of SP by semipreparative HPLC (Thermo Scientific Ultimate 3000) under the following conditions: HPLC using a reversed-phase C8 column (150 × 2.1 mm), solvents were 0.2% aqueous TFA (A) and 0.2% TFA in ACN/water 80/20 (v/v) (B). The gradient used was linear from 10% to 40% B in 60 min at a flow rate of 0.30 ml/min. Detection of salivary proteins was performed at 214 nm.

The different fractions of salivary proteins were freeze-dried, and the major families present in each fraction were identified by ESI-MS using flow injection analysis in an LTQ Orbitrap XL mass spectrometer (Thermo Fischer Scientific, Bremen, Germany) controlled by LTQ Tune Plus 2.5.5 and Xcalibur 2.1.0. The capillary voltage for electrospray ionization (ESI) was set at 3100 V. The capillary temperature was 275 °C. The flow rate of the sheath gas (nitrogen) was set to 5 (arbitrary unit according to software settings). The capillary voltage was 36 V, and the tube lens voltage was 110 V.

Samples were diluted 1:10 in a methanol/acetonitrile/TFA 0.01% (5:5:90 v/v) mixture before analysis. Because proteins assume different charge states at the interface, spectra were subjected to a deconvolution process using the charge ratio analysis method after mass spectrometric analysis with *MagTran* 1.03 software. The study was performed in accordance with the Declaration of Helsinki and submitted to the Ethics Committee.

2.5. Design of biosensor Au-SPE

The biosensor on designed on the working electrode (WE) area of the SPE, as shown in Fig. 1. Briefly, the WE was of gold and cleaned by washing with ethanol and milli-Q water and electrochemically cleaned with H_2SO_4, 0.5 mol/L, by CV, from 0. V to + 1.2 V, cycling voltage at 50 mV/s. Then, a thiol compound (25 mmol/L) solution was casted on the working electrode area for 2 h (Cys, L-cysteine or TA), and then washed with de-ionized water several times and kept in α-amylase (0.25 mg/mL) or PRP (0.25 mg/mL) prepared in PBS buffer, pH 7.4 and 5.0. The electrode was then rinsed thoroughly with milli-Q water to remove un-reacted species.

The immobilization steps of the electrode assembly were monitored by EIS and CV. EIS was performed from 10^{5} to 10^{-1} Hz, along 50 frequencies, with an amplitude of 0.01 V. CV was performed with a potential ranging from −0.6 V to 0.6 V, at a scan-rate of 50 mV/s.

2.6. Electrochemical assays

CV, EIS and square-wave voltammetry (SWV) measurements were performed in 5.0 mmol/L $[Fe(CN)_6]3-$ and 5.0 mmol/L $[Fe(CN)_6]^{4-}$ in PBS buffer pH 7.4 and pH 5.0, respectively (pH was adjusted by addition of phosphoric acid). At CV, the potential was scanned from −0.6 to + 0.6 V at 50 mV/s. For SWV studies, potentials were scanned from −0.4 to + 0.6 V, corresponding to a frequency of 10 Hz and a step height of 2.50 mV. EIS studies were performed with the same redox couple $[Fe(CN)_6]^{3-/4-}$ at a standard potential of 0.12 V, using an amplitude of 0.01 V RMS and a number of frequencies corresponding to the OCP value at 120 s and logarithmically distributed over a frequency range of 0.1–100 kHz. Impedance data were fitted to an electrochemical circuit using Nova software from Autolab (Metrohm). All tests were performed in triplicate.

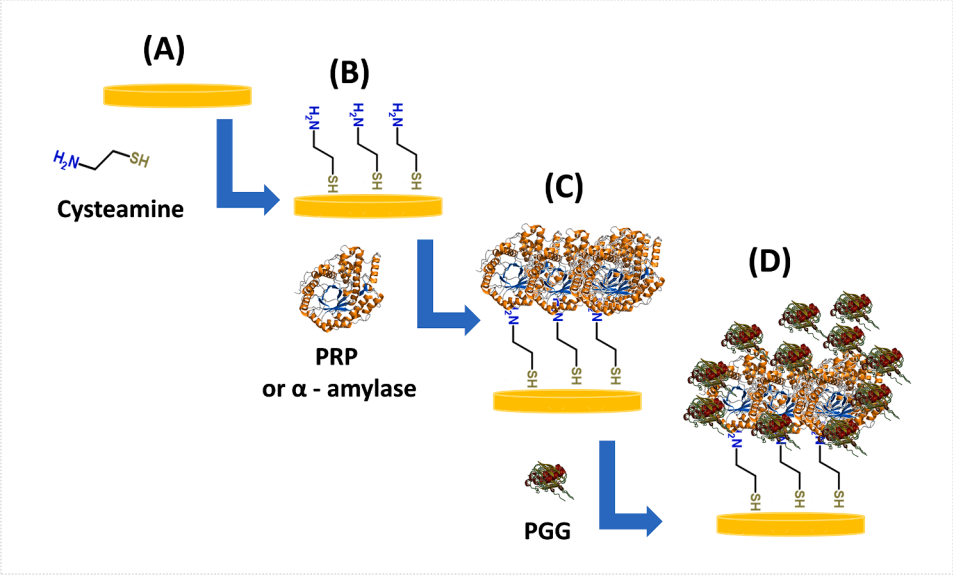

Fig. 1. Schematic representation of the sensing area on the biosensor. The gold working electrode (A) was modified with cysteamine (in the optimized version), which bound to the gold via the − SH group (B); the salivary proteins were then added to adsorb to the amine layer (C) and these would bind to the PGG polyphenols in food.

2.7. Analytical performance of the biosensor

The performance of the biosensor was checked in PGG standard solutions prepared in PBS buffer, and calibration was performed at room temperature by EIS. Assays were made at pH 5.0 and 7.4, in triplicate. The affinity of salivary proteins on the biosensor for other representative polyphenols in wines was also evaluated. GA was used for this purpose because it is a tannin that is highly represented in beverages and foods (Newsome, Li, & van Breemen, 2016). The solution was prepared in PBS buffer and the interaction between the compound and salivary proteins was followed by EIS and SWV measurements at room temperature. Interference by other minor compounds was also evaluated. The concentrations of the interfering compounds were chosen according to the amounts present in the wine. These included glucose (15%), fructose (15%), ethanol (16%), and glycerol (0.1%). All tests were performed in triplicate.

3. Results and discussion

The behaviour of the biosensor depends on several variables that require systematic evaluation by univariate optimization. The influence of the chemical composition of the monolayers, the family of salivary proteins, the pH and the concentration range of PGG were optimized. The main analytical properties and optimal working conditions were determined for both protein sensors prepared with PRP or α-amylase. The biosensor was synthesized in two main steps: (i) a thiol-based monolayer and (ii) a salivary protein layer, as explained below.

3.1. Thiol layer

The WE of Au-SPE was first modified by the formation of a monolayer, which has the more suitable chemical function and spatial organization to bind salivary proteins. The compound added for this purpose had a thiol group that binds quickly and tightly to the gold substrate (Fig. 1). This compound would also have specific chemical functions that would be exposed to the upper surface upon thiol binding to the gold electrode. These chemical functions included an amine group (Cys) or amine/carboxylic acid groups (L-cysteine) or two carboxylic acid groups (TA). At this stage, we were looking for the larger electrical difference between the gold and gold/monolayer signal. For this purpose, an incubation time of 1, 2, or 3 h or overnight was established. In general, a stable electrochemical signal was obtained after 2 h of incubation, so the following studies were performed at 2 h of incubation.

The electrical changes that occurred in the WE region after each stage of chemical modification or calibration were measured by CV and EIS. In EIS, data was collected in the form of Nyquist plots reflecting the physicochemical processes at the WE and modelled by the Randle's equivalent circuit (Tran, Son, & Min, 2016). In CV, data was collected in the form of voltammograms reflecting the current in WE when the potential was varied from negative to positive values and vice versa, resulting in reversible oxidation/reduction of the redox probe. Overall, the changes in peak current and potential at which each peak was observed reflected the changes in the intrinsic conductivity properties of the surface WE. The overall data obtained in this study is shown in Fig. 2.

The Nyquist plots of the pure Au-SPE gold showed a small semicircle region, indicating a fast charge transfer process with a diffusion-limiting step (Fig. 2). Addition of a thiol compound increased the Rct, reflected in the increased diameter of the semi-circular region of the Nyquist plot. Of the 3-thiol compounds tested, Cys was the one that showed a more intense difference to the blank measurement, with an Rct of 542 Ω (compared to TA with 271 Ω or L-cysteine with 252 Ω). Even with repeated measurements with different electrodes, Cys was the thiolate compound with the more stable and reproducible measurements. In general, the Rct values agreed well with the steric hindrances caused by the molecular structure of each compound for the redox probe. However, considering the charges of the chemical functions of Cys, TA, and L-cysteine after binding to WE, one would generally expect Cys to give a lower Rct value because it has an opposite charge to the redox probe. Thus, the higher Rct value of Cys also reflects its more effective binding to the WE surface. The data from CV were in complete agreement with the EIS data, indicating lower currents when the Rct value was higher. Overall, these results suggest that Cys should be used for the modification of the WE (Cys/Au-SPE) and casting of salivary proteins.

3.2. Effect of protein binding

Immobilization of α-amylase or PRP on Cys/Au-SPE was achieved by ionic/electrostatic interaction between the negatively charged groups or negatively polarized atoms of the proteins and the positively charged primary amine groups of Cys. According to typical protocols for protein binding, salivary proteins were incubated overnight at 4 °C on the Cys/Au-SPE. The electrode was then washed with MiliQ water to remove non-adsorbed proteins.

In general, the binding of salivary proteins provided an additional barrier to the access of the redox probe to the gold surface, as indicated by the increasing Rct values observed in Fig. 3. The average ΔΩ-value after α-amylase incubation was 151 Ω and after PRP incubation was 186 Ω. While these values seem different, the background differences obtained from the commercial electrodes do not show significant difference between the immobilization profiles of both proteins. Thus, the following studies were performed with biosensors assembled with the two proteins.

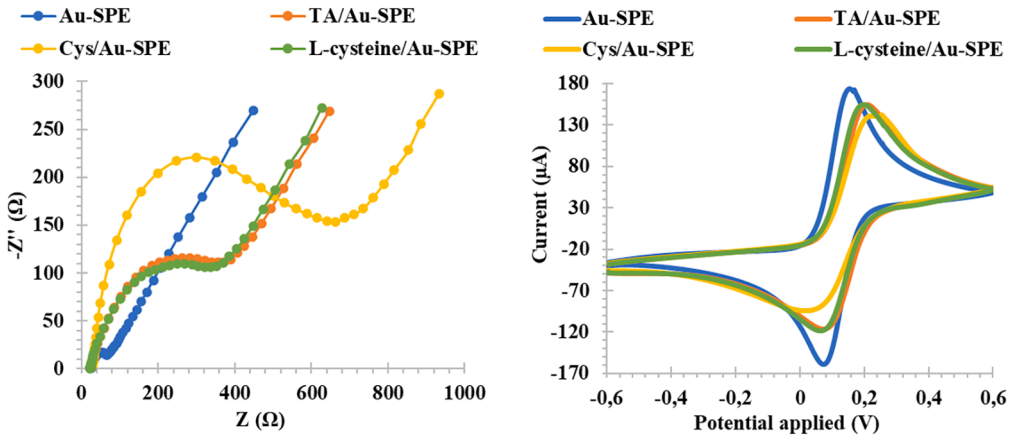

Fig. 2. Typical Nyquist plots (left) and voltammograms (right) of Au-SPE electrodes modified with different thiol compounds: cysteamine (Cys/Au-SPE), thiomalic acid (TA/Au-SPE) or L-cysteine (L-cysteine/Au-SPE).

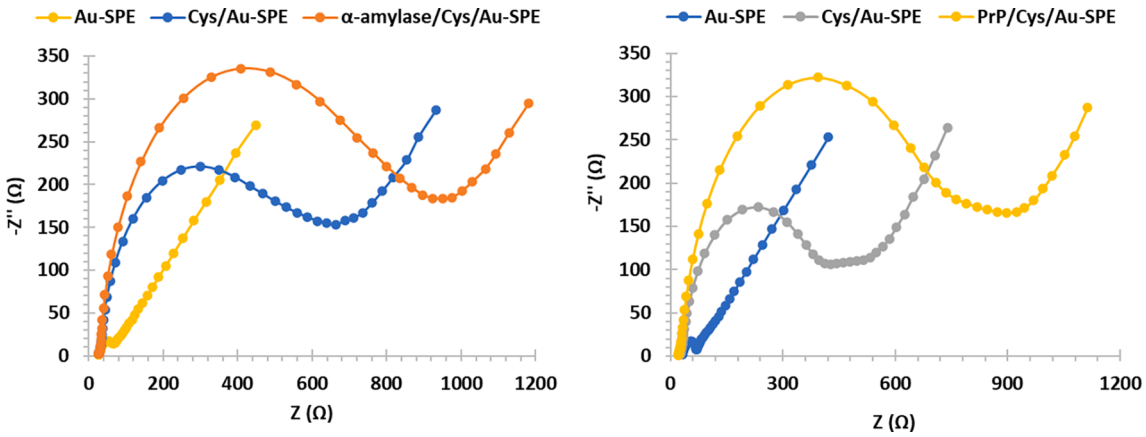

Fig. 3. Typical Nyquist plots of Au-SPE and the modified surfaces with Cys (Cys/Au-SPE) and α-amylase (α-amylase/Cys/Au-SPE, left) or PRP (PRP/Cys/Au-SPE, right).

3.3. pH dependence of the biosensor response

Calibrations were followed by EIS after incubation of PGG standard solutions at room temperature, from the lowest to the highest concentration, ranging from 0.11 μM to 5.3 μmol/L, and prepared in PBS at pH 5.0 or 7.4. Data was fitted as before, using the Rct equivalent semi-circle.

3.3.1. α-amylase biosensor

Nyquist plots obtained from the calibration curves are shown in Fig. 4-A1/B1. Data were plotted as PGG concentration versus Rct relative to the blank. The blank corresponded to the consecutive incubation of PBS solution until Rct readings showed negligible variation. The analytical performance of α-amylase/Cys/Au-SPE was significantly better when solutions were prepared at pH 5.0, compared with results obtained in solutions at pH 7.4. At pH 5.0, the sensor showed an average slope of 0.31 relative signal/μmol/L, squared correlation coefficients > 0.98 and a linear range from 0.1 to 4.4 μmol/L (Fig. 4B2). In contrast, calibrations at pH 7.4 (Fig. 4A2) showed a narrower concentration range of linear response and lower sensitivity, as reflected by a 3.3 × lower slope.

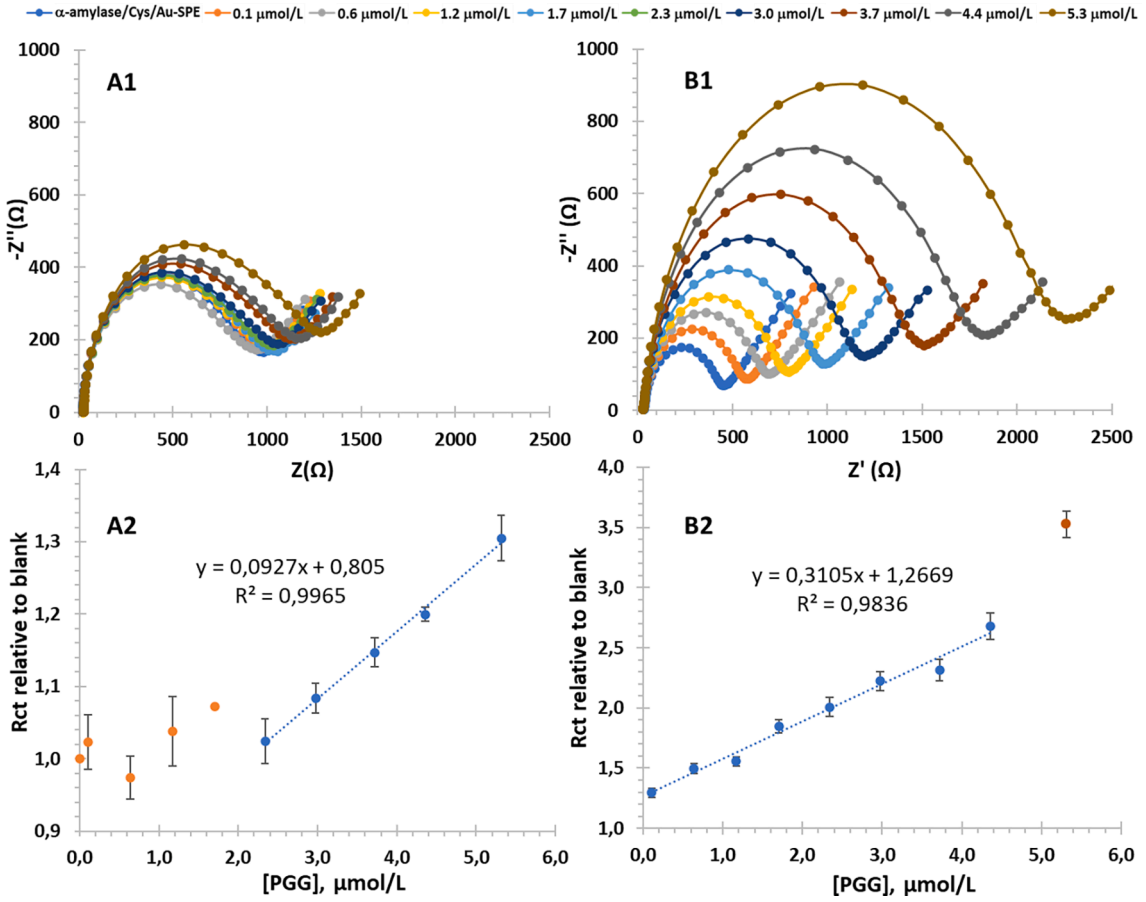

Fig. 4. Typical Nyquist plots obtained through the calibration of α-amylase/Cys/Au-SPE biosensor, for increasing concentrations of PGG standard solutions, up to 5.3 μmol/L, prepared in pH 7.4 (A1) and pH 5.0 (B1), along with the corresponding calibrations (A2 and B2, respectively).

Overall, these results showed that decreasing pH values increased the sensitivity of the calibration curve. This could be related to the increasing number of positive charges of the α-amylase structure at pH 5.0, since its isoelectric point is at 6.5 (Omichi & Ikenaka, 1988). The more positive the α-amylase is, the more strongly the PGG is attracted to it because it contains polyphenol structures that contain many − OH functions that are more strongly attracted to this positively charged PGG at pH 5 (than to the negatively charged PGG at pH 7.4). In addition, the redox probe is negatively charged, which means that it is naturally attracted to the PGG surface unless it is bound to the α-amylase. The stronger the PGG binding of the α-amylase, the stronger the Rct increase produced by the redox probe. Thus, it became clear 0that at a pH of 5.0, the amount of PGG bound to the surface is greater than at a pH of 7.4, making the analytical measurement more sensitive at a pH of 5.0.

3.3.2. PRP biosensor

The Nyquist plots of the curves of the PRP/Cys/Au-SPE biosensor are shown in Fig. 5-A1/B1, having calibration curves plotted as PGG concentration against the Rct relative to the blank signal (as established for the α-amylase biosensor). As for α-amylase, the biosensor displayed increasing Rct values for increasing PGG concentrations. Overall, the best calibration features were obtained for pH 5.0 (Fig. 5-B2), with average slopes of 0.56 relative Rct/μmol/L, squared correlation coefficients > 0.99 and a lower limit of linear range (LLLR) of 0.64 μmol/L. In opposite, calibrations in pH 7.4 (Fig. 5-A2), showed average slopes of 0.23 relative signal/μmol/L (half sensitivity when compared to pH 5.0), with squared correlation coefficients > 0.99 and a lower limit of linear range (LLLR) of 0.6 μmol/L.

Comparing the results of the α-amylase/Cys/Au-SPE and PRP/Cys/Au-SPE biosensors, it seems evident that the binding between PRP and PGG occurs with a higher affinity than the binding between α-amylase and PGG. This is in general agreement with the literature. PGG interacts linearly (one-to-one) with α-amylase via aromatic amino acid residues but forms complexes with acidic PRPs, which are crucial for astringency (Gyemant et al., 2009; S. Soares, Mateus, & de Freitas, 2012). However, in terms of biosensor response, the differences between the two devices made with the two salivary proteins did not allow to decide which one could be the best option to procced with further experiments. Therefore, the following studies will also be performed with both biosensors, PRP and amylase.

3.4. Affinity to gallic acid and catechin

In order to better understand the properties of the biosensor in relation to the response to astringent compounds and to validate the results obtained, other tannins were tested besides PGG. GA is a polyphenol commonly found in food matrices and coexists with PGG. The same is true for catechin. The results of the corresponding calibration curves obtained for the α-amylase/Cys/Au-SPE and PRP/Cys/Au-SPE biosensors are shown in Fig. 6A.

Interestingly, the Rct values obtained with GA and catechin solutions were too low, indicating that the binding affinity of the protein to these polyphenols was low. This suggested that the sensor surfaces were hardly able to form nonspecific bonds because the polyphenols were not "recognized" by the biosensors. It is important to mention that the signals shown in Fig. 6 were obtained with concentrations 40 times higher than the usual concentrations in real samples. When calibrated with these biosensors, the lower limits of the linear range (for these small changes in Rct) were 10 times lower for GA and 100 times lower for catechin (compared to PGG), regardless of the use of the α-amylase/Cys/

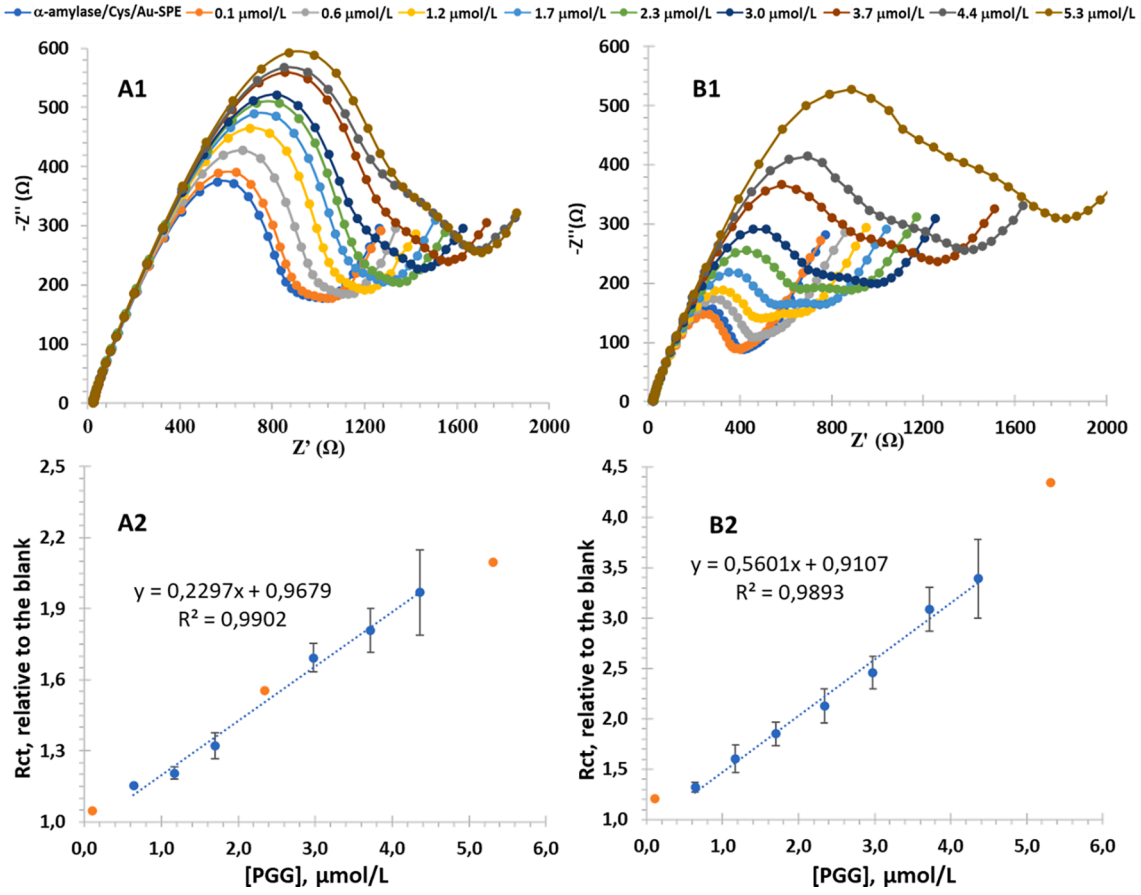

Fig. 5. Typical Nyquist plots obtained through the calibration of PRP/Cys/Au-SPE biosensor, for increasing concentrations of PGG standard solutions, up to 5.3 μmol/L, prepared in pH 7.4 (A) and pH 5.0 (B), along with the corresponding calibrations (A1 and B1, respectively).

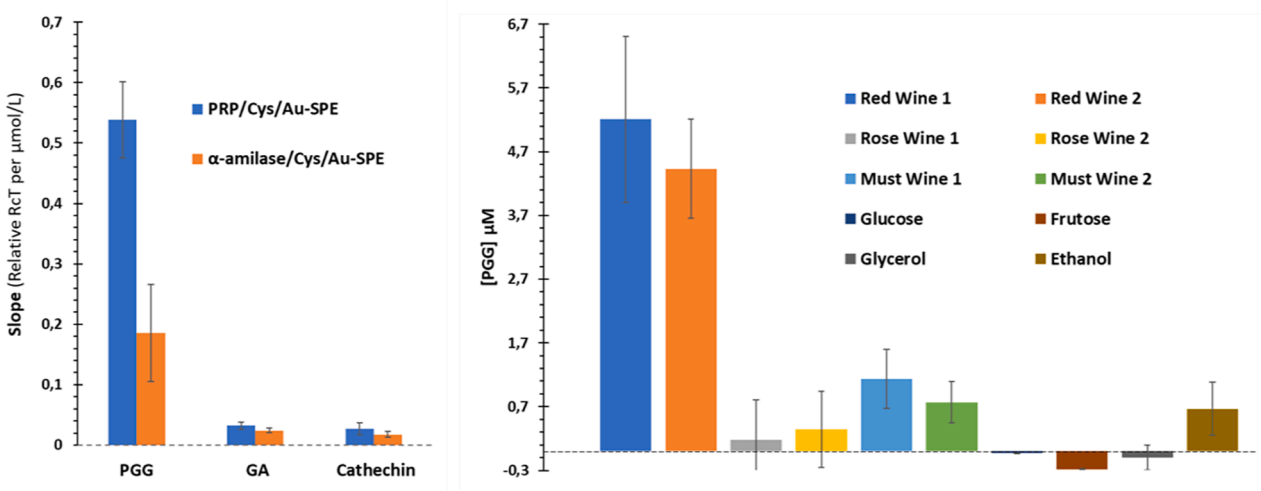

Fig. 6. (A) Signal change of the α-amylase/Cys/Au-SPE and PRP/Cys/Au-SPE biosensors after incubation with different concentrations of PGG, GA or catechin solutions, in PBS, at pH 5.0. (B) Wine samples (red wines, musts and rose) and wine interfering species (glucose, fructose, glycerol, and ethanol), 100 × diluted with PBS buffer, at pH 5.0. (For interpretation of the references to colour in this figure legend, the reader is referred to the web version of this article.)

Au-SPE or PRP/Cys/Au-SPE biosensor.

Overall, this data confirmed that the affinity of PGG to the salivary proteins α-amylase or PRP is much higher than that of GA or catechin. Thus, since the interaction of polyphenols with salivary proteins is considered a key mechanism for astringency perception, PGG can be postulated as a major contributor to astringency. This was already expected and suggested the possibility of testing the biosensor in food samples.

3.5. Real samples analysis and selectivity

Having in mind the possibility of getting relevant information in terms of astringent compounds with the biosensors developed, several wine samples were analysed by the electrochemical biosensors developed herein. Measurements were performed in triplicate to ensure good reproducibility and representativity of the reported data. The average data so obtained is shown in Fig. 6B. The triplicate data for each sample analysed corresponds to the same sample at different time days with different sensing units.

To prove the concept, we tested the response of the PRP biosensor to polyphenol-rich beverages (red wine, must wine and rose wine, two for each kind) and the possible interference by coexisting species in wines (glucose, fructose, glycerol and ethanol). The wine samples were numbered according to untreated wines (1) and the same wines treated with a commercial yeast protein extract fining agent (2) (YPE, Divino®), belonging to three different categories: (i) red wine, which is typically highly astringent (red wines 1 and 2); (ii) must wine, which is typically low astringent (must wines 1 and 2); (iii) and rose wine, which is not astringent (rose wine 1 and 2). The treatment applied is currently used in winemaking to stabilize the wine and reduce astringency and bitterness. Although these categories correspond to the general perception of astringency, it is important to note that all wines tested were part of an astringency sensory study (Figure S1, Supplementary Data, Wine Expert Sensory Panel of Divino®) and samples were classified into these relative orders of astringency.

All samples were diluted 100 × in PBS with a pH of 5.0 so that the sample analysis matched the calibration curve obtained (preliminary tests were performed with the more concentrated wines to determine the best dilution ratio). Each diluted sample was then incubated on the electrode for 30 min at room temperature. Then, the sample solution was replaced by the redox probe, to collect the corresponding EIS data. The Rct data were used to calculate the concentration values in the sample, expressed in PGG, by using the typical linear trend of the calibration curves obtained under the same conditions. The calculated data are shown in the bar graph in Fig. 6B. The standard deviation for two measurements of the same wine made on different days and with different biosensors was always less than 10%. In general, the relative data obtained were in complete agreement with the information available for these samples. The red wine showed a 2.6-fold higher response than the must wine, while the rose wines gave residual values. The biosensor response obtained for the different wines agreed with the sensory data (Figure S1, Supplementary Data). Considering untreated wines, Red wine 1 was the one with the highest astringency perception, followed by must wine 1 and then rosé wine, in correspondence with the biosensor response. Furthermore, samples of red wine and must wine that were treated with the finning agent had a decreased astringency perception (untreated samples are identified as #1 and treated samples are #2). This decreasing astringency perception was more evident for red wine, as expected. Rose wine treated with the finning agent had a slight increase in astringency perception, but this was not significant as the value obtained nears the limit of detection. These changes in astringency perception were consistent with the biosensor response.

Glucose (7% to 15%), fructose (7% to 15%), ethanol (12% to 16%), and glycerol (0.04% to 0.1%) were selected to study the effects of non-polyphenolic compounds commonly found in alcoholic beverages (Fig. 6B). As before, solutions of these compounds were prepared in PBS at pH 5.0 and tested in PRP biosensors to monitor the effects of the sample matrix. Overall, the maximum PGG concentration produced by these compounds was approximately 0.7 µmol/L [PGG] equivalents. This means that any values above 1.0 µmol/L [PGG] equivalents were due to astringent compounds alone. Thus, this limit can be considered as the detection limit for the determination of astringent polyphenols in wine samples.

Overall, the biosensor results agreed well with the sensory analysis data, which is also consistent with what should be expected for wine quality and astringency perception. Importantly, the sensitivity of the monitoring system for astringent compounds was incredibly much higher than conventional sensory panels, as the more concentrated samples had to be diluted 100-fold. This aspect could be particularly relevant for samples with low astringency, which can be more accurately monitored (stratified) with the proposed electrochemical biosensors, provided that the dilution level is kept in a lower value.

4. Conclusions

The biosensors developed herein have shown the ability to monitor

astringent compounds in beverages by replicating the binding event between salivary proteins and polyphenols on an electrochemical platform. The electrode setup was very simple and consisted only of binding the salivary proteins, PRPs or α-amylase, to an electrochemical transducer of gold and amine. Binding to the polyphenols PGG at a pH of 5.0 was sensitive in the range of 0.1 to 4.4 μmol/L, as determined by tracking a standard redox by EIS. This work was validated by successful polyphenol calibrations using EIS and SWV measurements, which were also used to monitor wine samples. Analytical application to wines proved successful for the PRP-based biosensors. In fact, the astringent polyphenol content estimated by the biosensor showed good correlation with the values determined by the sensory panel.

The resulting devices may open new doors to understanding the chemical/physical properties of this binding process for other groups of compounds, thus expanding the possibilities for astringency studies. In fact, the designing of similar biosensing devices with different salivary proteins may provide relevant information to the understanding of astringency. The electrochemical biosensor has the advantage over other conventional methods in that it is simple, has a short detection time, and does not interfere with other common compounds in wine. Therefore, we believe that this biosensor device is valuable for real-time monitoring of astringent compounds in the wine industry, when needed.

CRediT authorship contribution statement

Joana J. Costa: Investigation, Data curation, Visualization, Validation, Writing – original draft. **Felismina T.C. Moreira:** Investigation, Methodology, Data curation, Visualization, Validation, Supervision, Resources, Writing – original draft. **Susana Soares:** Funding acquisition, Validation, Visualization, Writing – review & editing. **Elsa Brandão:** Visualization, Writing – review & editing. **Nuno Mateus:** Visualization, Writing – review & editing. **Victor De Freitas:** Conceptualization, Funding acquisition, Validation, Visualization, Resources, Writing – review & editing. **M. Goreti F. Sales:** Conceptualization, Funding acquisition, Methodology, Visualization, Validation, Supervision, Resources, Writing – review & editing.

Declaration of Competing Interest

The authors declare that they have no known competing financial interests or personal relationships that could have appeared to influence the work reported in this paper.

Acknowledgements

FoodNanoSense, *Compreensão do amargor e adstringência dos polifenóis presentes em alimentos para o desenvolvimento de um biossensor*, supported by Fundação para a Ciência e Tecnologia, with reference PTDC/AGR-TEC/6547/2014.

Appendix A. Supplementary data

Supplementary data to this article can be found online at https://doi.org/10.1016/j.foodchem.2022.133587.

References

Bate-Smith, E. C., & Swain, T. (1962). *Flavonoid compounds*. New York: Academic Press.

Breslin, P. A. S., Gilmore, M. M., Beauchamp, G. K., & Green, B. G. (1993). Psychophysical evidence that oral astringency is a tactile sensation. *Chemical Senses, 18*(4), 405–417. https://doi.org/10.1093/chemse/18.4.405

Canon, F., Neiers, F., & Guichard, E. (2018). Saliva and Flavor Perception: Perspectives. *Journal of Agricultural and Food Chemistry, 66*(30), 7873–7879. https://doi.org/10.1021/acs.jafc.8b01998

Canon, F., Paté, F., Cheynier, V., Sarni-Manchado, P., Giuliani, A., Pérez, J., … Cabane, B. (2013). Aggregation of the Salivary Proline-Rich Protein IB5 in the Presence of the Tannin EgCG. *Langmuir, 29*(6), 1926–1937. https://doi.org/10.1021/la3041715

Chen, Y. M., Hagerman, A. E., & Minto, R. E. (2003). Preparation of 1,2,3,4,6-penta-O-galloyl- U-C-14 -D-glucopyranose. *Journal of Labelled Compounds & Radiopharmaceuticals, 46*(1), 99–105. https://doi.org/10.1002/jlcr.648

Cory, H., Passarelli, S., Szeto, J., Tamez, M., & Mattei, J. (2018). The Role of Polyphenols in Human Health and Food Systems: A Mini-Review. *Frontiers in nutrition, 5*, 87-87. https://doi.org/10.3389/fnut.2018.00087.

Davies, H. S., Pudney, P. D. A., Georgiades, P., Waigh, T. A., Hodson, N. W., Ridley, C. E., … Thornton, D. J. (2014). Reorganisation of the Salivary Mucin Network by Dietary Components: Insights from Green Tea Polyphenols. *PLOS One, 9*(9), e108372.

de Wijk, R. A., & Prinz, J. F. (2005). The role of friction in perceived oral texture. *Food Quality and Preference, 16*(2), 121–129. https://doi.org/10.1016/j.foodqual.2004.03.002

Goldberg, E., Grant, J., Aliani, M., & Eskin, M. N. A. (2017). Methods for Removing Bitterness in Functional Foods and Nutraceuticals. *In Bitterness*, 209–237.

Guerreiro, J. R. L., Frederiksen, M., Bochenkov, V., Freitas, V., Sales, M. G. F., & Sutherland, D. S. (2014). Multifunctional Biosensor Based on Localized Surface Plasmon Resonance for Monitoring Small Molecule–Protein Interaction. *ACS Nano, 8*(8), 7958–7967. https://doi.org/10.1021/nn501962y

Guerreiro, J. R. L., Freitas, V., Sutherland, D. S., & Sales, M. G. F. (2012). SPR based Studies for Pentagalloyl Glucose Binding to α-Amylase. *Procedia Engineering, 47*, 498–501. https://doi.org/10.1016/j.proeng.2012.09.193

Guerreiro, J. R. L., Sutherland, D. S., Freitas, V., & Sales, M. G. F. (2013). Protein–polyphenol interaction on silica beads for astringency tests based on eye, photography or reflectance detection modes. *Analytical Methods, 5*, 2694–2703. https://doi.org/10.1039/C3AY26478E

Guerreiro, J. R. L., Teixeira, N., Freitas, V., Sales, M. G. F., & Sutherland, D. S. (2017). A saliva molecular imprinted localized surface plasmon resonance biosensor for wine astringency estimation. *Food Chemistry, 233*, 457–466. https://doi.org/10.1016/j.foodchem.2017.04.051

Gyemant, G., Zajacz, A., Becsi, B., Ragunath, C., Ramasubbu, N., Erdodi, F., … Kandra, L. (2009). Evidence for pentagalloyl glucose binding to human salivary alpha-amylase through aromatic amino acid residues. *Biochimica Et Biophysica Acta-Proteins and Proteomics, 1794*(2), 291–296. https://doi.org/10.1016/j.bbapap.2008.10.012

Huang, R., & Xu, C. (2021). An overview of the perception and mitigation of astringency associated with phenolic compounds. *20*(1), 1036-1074. https://doi.org/https://doi.org/10.1111/1541-4337.12679.

Liem, D. G., Miremadi, F., & Keast, R. S. J. (2011). Reducing Sodium in Foods: The Effect on Flavor. *Nutrients, 3*(6), 694–711. https://doi.org/10.3390/nu3060694

Ma, W., Guo, A., Zhang, Y., Wang, H., Liu, Y., & Li, H. (2014). A review on astringency and bitterness perception of tannins in wine. *Trends in Food Science & Technology, 40*(1), 6–19. https://doi.org/10.1016/j.tifs.2014.08.001

Meyerhof, W., Batram, C., Kuhn, C., Brockhoff, A., Chudoba, E., Bufe, B., … Behrens, M. (2010). The molecular receptive ranges of human TAS2R bitter taste receptors. *Chemical Senses, 35*(2), 157–170. https://doi.org/10.1093/chemse/bjp092

Meyerhof, W., Born, S., Brockhoff, A., & Behrens, M. (2011). Molecular biology of mammalian bitter taste receptors. A review. *Flavour and Fragrance Journal, 26*(4), 260–268. https://doi.org/10.1002/ffj.2041

Nadathur, S. R., & Carolan, M. (2017). Chapter 23 - Flavors, Taste Preferences, and the Consumer: Taste Modulation and Influencing Change in Dietary Patterns for a Sustainable Earth. In S. R. Nadathur, J. P. D. Wanasundara, & L. Scanlin (Eds.), *Sustainable Protein Sources* (pp. 377–389). San Diego: Academic Press.

Newsome, A. G., Li, Y. C., & van Breemen, R. B. (2016). Improved Quantification of Free and Ester-Bound Gallic Acid in Foods and Beverages by UHPLC-MS/MS. *Journal of Agricultural and Food Chemistry, 64*(6), 1326–1334. https://doi.org/10.1021/acs.jafc.5b04966

Omichi, K., & Ikenaka, T. (1988). Separation of human salivary alpha-amylase isozymes by high-performance liquid-chromatography with a continuous monitor system of the activity. *Analytical Biochemistry, 168*(2), 332–336. https://doi.org/10.1016/0003-2697(88)90326-0

Ployon, S., Morzel, M., Belloir, C., Bonnotte, A., Bourillot, E., Briand, L., … Canon, F. (2018). Mechanisms of astringency: Structural alteration of the oral mucosal pellicle by dietary tannins and protective effect of bPRPs. *Food Chemistry, 253*, 79–87. https://doi.org/10.1016/j.foodchem.2018.01.141

Quijada-Morín, N., Crespo-Expósito, C., Rivas-Gonzalo, J. C., García-Estévez, I., & Escribano-Bailón, M. T. (2016). Effect of the addition of flavan-3-ols on the HPLC-DAD salivary-protein profile. *Food Chemistry, 207*, 272–278. https://doi.org/10.1016/j.foodchem.2016.03.118

Roland, W. S. U., van Buren, L., Gruppen, H., Driesse, M., Gouka, R. J., Smit, G., & Vincken, J.-P. (2013). Bitter Taste Receptor Activation by Flavonoids and Isoflavonoids: Modeled Structural Requirements for Activation of hTAS2R14 and hTAS2R39. *Journal of Agricultural and Food Chemistry, 61*(44), 10454–10466. https://doi.org/10.1021/jf403387p

Schöbel, N., Radtke, D., Kyereme, J., Wollmann, N., Cichy, A., Obst, K., … Hatt, H. (2014). Astringency Is a Trigeminal Sensation That Involves the Activation of G Protein-Coupled Signaling by Phenolic Compounds. *Chemical Senses, 39*(6), 471–487. https://doi.org/10.1093/chemse/bju014

Silva, M. S., García-Estévez, I., Brandão, E., Mateus, N., de Freitas, V., & Soares, S. (2017). Molecular interaction between salivary proteins and food tannins. *Journal of Agricultural and Food Chemistry, 65*(31), 6415–6424. https://doi.org/10.1021/acs.jafc.7b01722

Soares, S., Brandão, E., Mateus, N., & de Freitas, V. (2017). Sensorial properties of red wine polyphenols: Astringency and bitterness. *Critical Reviews in Food Science and Nutrition, 57*(5), 937–948. https://doi.org/10.1080/10408398.2014.946468

Soares, S., Kohl, S., Thalmann, S., Mateus, N., Meyerhof, W., & De Freitas, V. (2013). Different Phenolic Compounds Activate Distinct Human Bitter Taste Receptors.

Journal of Agricultural and Food Chemistry, 61(7), 1525–1533. https://doi.org/10.1021/jf304198k

Soares, S., Mateus, N., & de Freitas, V. (2012). Interaction of different classes of salivary proteins with food tannins. *Food Research International, 49*(2), 807–813. https://doi.org/10.1016/j.foodres.2012.09.008

Soares, S., Soares, S., Brandão, E., Guerreiro, C., Mateus, N., & de Freitas, V. (2020). Oral interactions between a green tea flavanol extract and red wine anthocyanin extract using a new cell-based model: Insights on the effect of different oral epithelia. *Scientific Reports, 10*(1), 12638. https://doi.org/10.1038/s41598-020-69531-9

Soares, S., Vitorino, R., Osório, H., Fernandes, A., Venâncio, A., Mateus, N., … de Freitas, V. (2011). Reactivity of human salivary proteins families toward food polyphenols. *Journal of Agricultural and Food Chemistry, 59*(10), 5535–5547. https://doi.org/10.1021/jf104975d

Tran, T. B., Son, S. J., & Min, J. (2016). Nanomaterials in Label-free Impedimetric Biosensor: Current Process and Future Perspectives. *Biochip Journal, 10*(4), 318–330. https://doi.org/10.1007/s13206-016-0408-0

Upadhyaya, J., Singh, N., Bhullar, R., & Chelikani, P. (2017). Biochemistry of Human Bitter Taste Receptors. *In Bitterness*, 1–20.

Yan, Q., & Bennick, A. (1995). Identification of histatins as tannin-binding proteins in human saliva. *Biochem J, 311*(Pt 1)(Pt 1), 341–347. https://doi.org/10.1042/bj3110341

Zhang, N., Wei, X., Fan, Y., Zhou, X., & Liu, Y. (2020). Recent advances in development of biosensors for taste-related analyses. *TrAC Trends in Analytical Chemistry, 129*, Article 115925. https://doi.org/10.1016/j.trac.2020.115925